**Proceedings of the ASME 2014 International Design Engineering Technical Conferences &
Computers and Information in Engineering Conference
IDETC/CIE 2014
August 17-20, 2014, Buffalo, New York, USA**

DETC2014-35310

A HARDWARE-IN-THE-LOOP PLATFORM
FOR A SERIES HYBRID POWERTRAIN
FEATURING TWO EQUIVALENT CONSUMPTION MINIMIZATION STRATEGIES

Sara Mohon
Clemson University
Greenville, SC, USA

Satadru Dey
Clemson University
Greenville, SC, USA

Beshah Ayalew
Clemson University
Greenville, SC, USA

Pierluigi Pisu
Clemson University
Greenville, SC, USA

ABSTRACT

Hardware-in-the-loop (HIL) platforms enable rapid evaluation of different system configurations and energy management strategies for electrified/hybrid powertrains without building full vehicle prototypes. This paper outlines a HIL platform for a series hybrid powertrain and discusses particular control strategies. The main hardware components of the platform are a gasoline generator, a lead acid battery pack, a bi-directional dc/dc converter, a programmable dc load, strain gauges, and a rotary encoder. Along with these hardware components, a real-time control prototyping system is used to implement energy management strategies and monitor several signals form the HIL platform. The effectiveness and performance of this platform is demonstrated by implementing two versions of the Equivalent Consumption Minimization Strategy (ECMS). The first version uses a constant equivalence factor for weighting the cost of electrical energy storage, while the second version uses an adaptive equivalence factor based on the deviation of battery state of charge (SOC) from a reference SOC.

INTRODUCTION

Electric and hybrid vehicles are becoming increasingly popular due to their promising reduction in noxious emissions and improved fuel economy [1]. However, the continued success of these technologies, particularly of hybrids, strongly depends on efficient utilization of multiple onboard energy sources. In general, under a hybrid configuration the split of power demand among multiple on-board sources can be decided to fulfill some optimality criteria targeting the minimization of fuel consumption and/or undesired emissions while meeting driver demanded performance and other system constraints. There are several energy management strategies proposed in the literature, including dynamic programming, rule-based, fuzzy logic, neural networks, and equivalent consumption minimization [2, 3, 4]. As an integral part of research and development, HIL can be a useful tool for rapid testing and evaluation of these different energy management strategies.

A HIL platform can be viewed as an intermediate step between computer simulation and building a full system prototype. It constitutes of a closed-loop environment with a combination of physical and virtual prototypes of the individual subsystems. The main advantage of a HIL setup is the capability of emulating the real scenario with a higher degree of fidelity than can be captured fully via software simulation only. Today, HIL setups are indispensable for cost effective rapid prototyping of systems in the aerospace, automotive and several other industries [5].

In the literature, several works can be found on the area of HIL testing of hybrid powertrains. In [6], a Diesel hybrid electric vehicle (HEV) HIL platform was built with hardware including a Diesel engine, a lead acid battery pack, and an electric machine. The resulting fuel consumption was compared to that of a conventional vehicle. Another Diesel HEV HIL platform was demonstrated in [7] including an ECMS strategy to reduce NOx emissions while still maintaining reduced fuel consumption. A gasoline HEV HIL platform was described in [8]. This platform was a parallel HEV configuration with gasoline engine, battery pack, and an electric machine. HIL testing can also focus on only one piece of hardware such as one electric motor and the rest of the HEV

is simulated in software. An example is given in [9], which describes HIL is used for electric motor prototyping inside an HEV design.

In this paper, we describe the layout and implementation of a series gasoline-electric HIL platform initially developed for educational and research purposes. Similar to the above works, typical usages of this platform include: 1) evaluation of different energy management strategies, 2) characterization of individual components of the powertrain. We illustrate the effectiveness and capability of the platform by demonstrating two versions of ECMS [4] implemented on this HIL platform. The ECMS strategy solves for the optimal split of power demand between the battery pack and the engine by minimizing an instantaneous cost that includes fuel consumption by the gasoline engine as well as associated penalties in sustaining or depleting charge in the battery via an equivalence factor. The two versions of ECMS we consider are: one with a constant equivalence factor and another with an adaptive equivalence factor. Both versions have been extensively illustrated via system software simulations in the literature [4,10,11,12]. This paper focuses on experimental implementations of the strategy on the HIL platform.

The remainder of the paper is organized as follows. First, we describe the details of the HIL platform. Then we discuss the control strategies as applied to this platform. This is followed by some experimental results from using these control strategies on the platform. Finally, we include some concluding remarks at the end of the paper.

PLATFORM DETAILS

The HIL platform for the series hybrid powertrain presented in this paper consists of several hardware and software tools. Figure 1 shows a picture of the setup. The main components consist of a 2.5 kW gasoline genset [13], a Werker 35Ah lead acid battery pack [14], two AC/DC converters [15], a bidirectional DC/DC converter from Zahn Inc. [16], an NHR 6kW DC load [17], strain gauges, and a rotary encoder [18]. A dSPACE 1104 board is used as the real-time data acquisition and control hardware. The control algorithm is built in MATLAB/Simulink and interfaced to dSPACE ControlDesk software for real-time experimentations.

The detail schematic of the HIL platform is shown in Figure 2. The series hybrid configuration consists of two separate energy sources: a battery pack and gasoline genset. The outputs from the gasoline genset are connected to two AC/DC converters that convert the 120VAC genset voltage to 48VDC voltage. The battery pack consists of three 12VDC lead acid batteries connected in series. The battery pack output is connected to a bi-directional DC/DC converter to allow discharging and charging of the battery pack. The DC/DC converter is a step-up converter that allows output voltage on the DC load side to vary between 38VDC and 60VDC. On the output power side of the DC/DC converter is a 1 Ω resistor. Then the DC power after the resistor and AC/DC converters is

fed to the DC load. The DC load emulates the current demand from the vehicle (driver) as commanded by the control system.
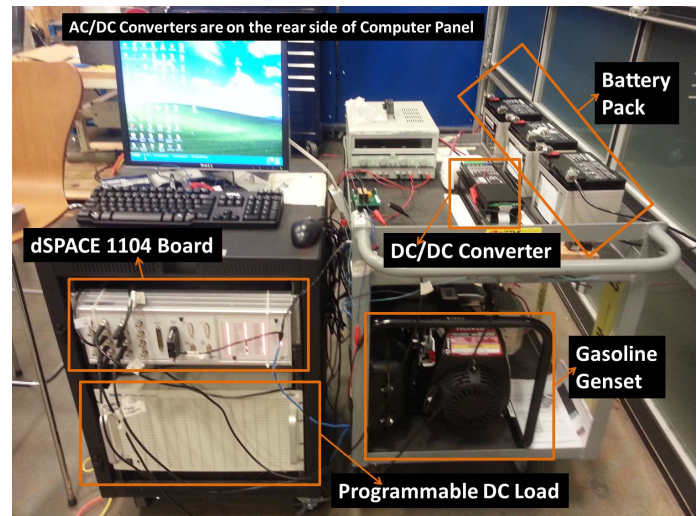

Figure 1: Series Hybrid Powertrain HIL Platform

Current measurement shunts are placed between the battery and DC/DC converter and also between the DC/DC converter and DC load. The current from the generator is calculated as the difference between DC load current and current shunt measurement between the DC/DC converter and DC load. The setup also includes strain gauges and a rotary encoder on the genset output for torque and speed measurement.

The power split in this platform is achieved by a control signal sent to the DC/DC converter. The converter operates only in voltage control mode with a voltage signal controlling the variable output voltage of the device. However, we prefer to operate the converter in current control mode and control the output current of the DC/DC converter since our ECMS objective function will reduce to a function of currents (see Control Strategy section below). By using the 1 Ω resistor after the converter, we can map the control voltage to the output current after the resistor. Based on the control voltage of the DC/DC converter, its output voltage varies between 38VDC to 60VDC while the load voltage remains constant at 48VDC. The voltage difference across the resistor determines the direction and output current of DC/DC converter accordingly. If the output voltage of the DC/DC converter is 38VDC and the load voltage is 48VDC then a current of 10A will flow from the DC load side through the resistor to the DC/DC converter to charge the battery pack. Therefore, the converter voltage signal determines the commanded current of the battery pack. The rest of the current demand will be automatically supplied by the self-regulated gasoline genset, which operates at a fixed speed.
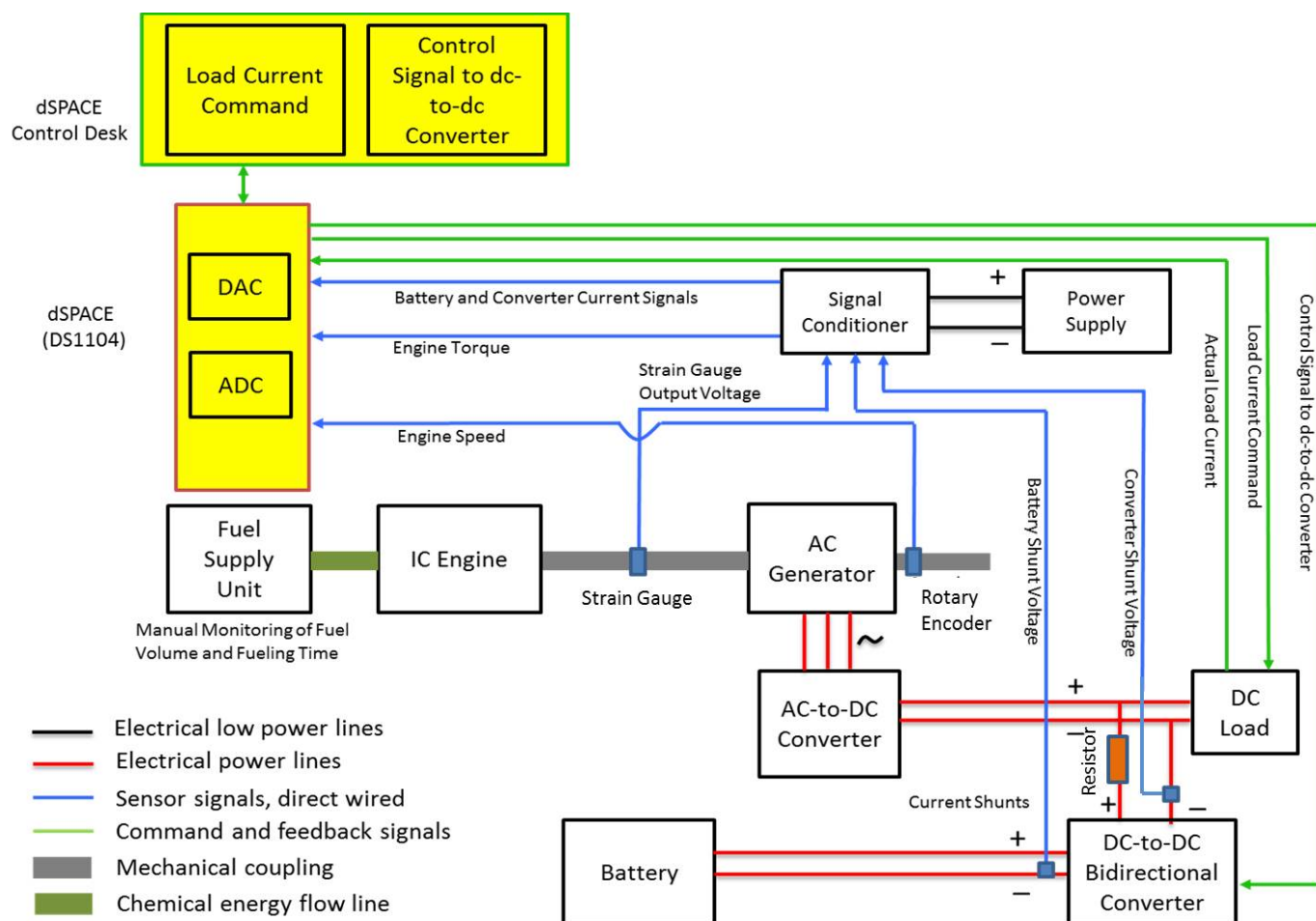
2

Copyright © 2014 by ASME

Figure 2: HIL Platform Schematic

COMPONENT MODELING
Gasoline Genset

An efficiency map of the 2.5kW gasoline genset operating at 3600rpm has been created using experimental current and fuel flow rate data. The efficiency map is shown in Figure 3. This map will be used in the control strategy.
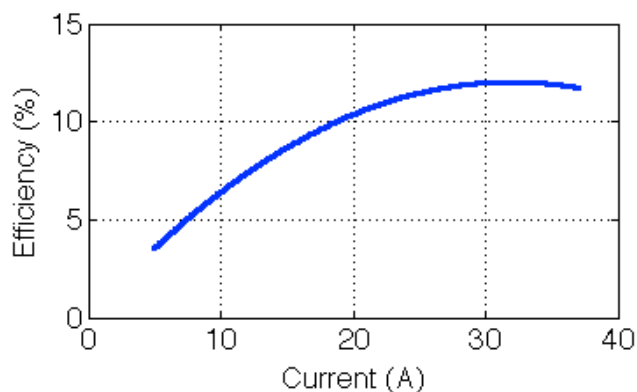

Figure 3: Gasoline Genset Fuel Efficiency Map

Battery Pack

A Thévenin equivalent circuit formulation is used to model the battery pack. The equivalent circuit used is shown in Figure 4.
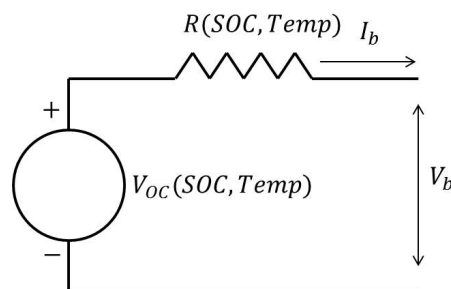

Figure 4: Battery Equivalent Circuit Model

The equivalent open circuit voltage source and resistance is modeled as a function of SOC as shown in Figure 5. These parameters were estimated using experimental data of the battery terminal voltage and current. While it is possible to

3   Copyright © 2014 by ASME

include temperature effects, that has not been done in this demonstration.
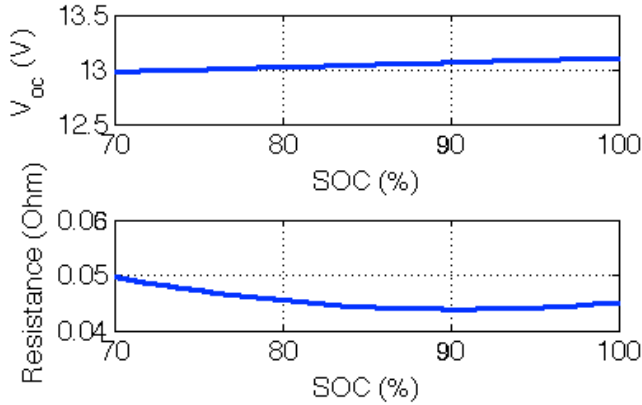

Figure 5: Battery Open Circuit Voltage and Resistance as a Function of SOC, at Temp= 25°C

DC/DC Converter

The DC/DC converter operates only in voltage control mode. The DC/DC converter output voltage changes based on a control signal given to it called V_{ref}. To convert it to a current control mode, a 1 Ω resistor has been added to the output of the DC/DC converter. Using this circuit configuration, a sequential map has been created to map the control signal to output voltage to output current. Essentially the map gives the relation between the control signal and the output current of the DC/DC converter in that particular configuration. The original map between control voltage and output voltage is shown in Figure 6. The efficiency of the DC/DC converter is assumed to be a constant 90% in the computations that follow.
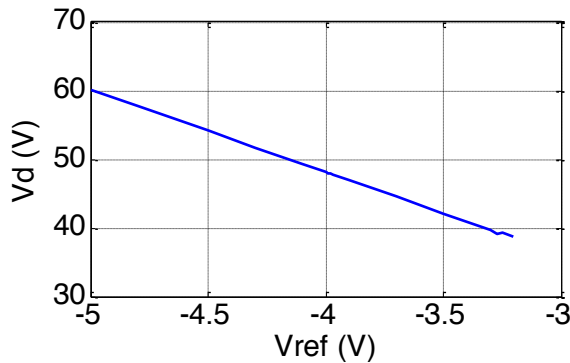

Figure 6: DC/DC Converter Control Signal to Output Voltage Map

Vehicle Model

The following vehicle parameters and equations have been chosen to convert the driving profile in velocity to a corresponding power requirement.

Parameter	Value	Unit
ρ	1.29	Kg/m^3
m	4350	Kg
g	9.18	m/s^2
C_d	0.43	-
A_f	2.9	m^2
C_{r0}	0.013	-
C_{r1}	0.007	-

Table 1: Vehicle Parameters

$$P_{req} = v\left(m_{eff}\frac{dv}{dt} + \frac{1}{2}A_f\rho C_d v^2 + mgC_r \right) \tag{1}$$

$$C_r = C_{r0} + C_{r1}\left(\frac{v_{kph}}{100}\right)^{2.5} \tag{2}$$

where v_{kph} is velocity in km/hr. Definitions of the various symbols is included in the nomenclature at the end of the paper.

CONTROL STRATEGY

A simplified schematic of the power flow in a series hybrid vehicle powertrain is shown in Figure 7. The vehicle is driven by an electric motor that is powered by the combination of two energy sources via an electrical summation. In our HIL setup, the power requirement by the electric motor to drive the vehicle is emulated by a programmable DC load. An ECMS strategy decides the split of power requirement between the sources based on the optimality criterion detailed below.
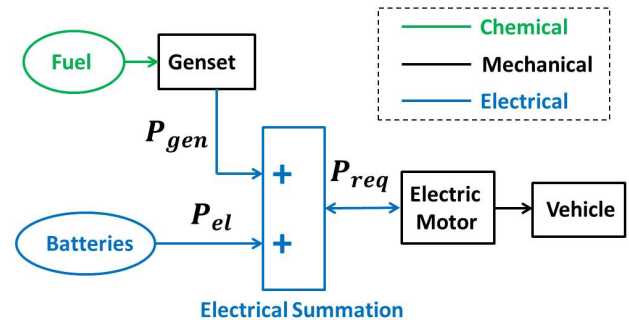

Figure 7: Schematic of Series Hybrid Powertrain Configuration

In ECMS, an objective function is formulated in order to minimize the equivalent fuel consumption of the vehicle subject to different constraints. The global minimization problem of fuel consumption can be written as

Copyright © 2014 by ASME

$$J = \min_{\{P_{gen}(t), P_{el}(t)\}} \int_0^T \dot{m}_{f,eq}(\tau)\, d\tau \qquad (3)$$

subject to
$$P_{req}(t) = P_{gen}(t) + P_{el}(t)$$
$$0 \le P_{gen}(t) \le P_{gen_{MAX}}$$
$$P_{el_{MIN}} \le P_{el}(t) \le P_{el_{MAX}}$$
$$0 < SOC_{\min} \le SOC \le SOC_{\max} \le 1$$

where P_{req} is the power requirement from the vehicle, P_{gen} is the genset power, P_{el} is the battery power and $\dot{m}_{f,eq}$ is the equivalent fuel flow rate of the vehicle. The equivalent fuel flow rate of the vehicle is a parameter related to the combined power consumption from the battery pack and the genset and is defined as

$$\dot{m}_{f,eq} = \frac{P_{req}}{Q_{LHV}} \qquad (4)$$

In ECMS, the global minimization is first converted to a local minimization forming a new instantaneous fuel consumption objective function (see [4]). Furthermore, in the present case, the load voltage is fixed at 48VDC. Therefore, the objective function and power constraints can be written in terms of (equivalent) currents, as follows:

$$\text{minimize } \dot{m}_{f,eq} = \dot{m}_{f,ICE}(I_g) + \dot{m}_{f,Batt,eq}(I_d) \qquad (5)$$

subject to
$$I_{load}(t) = I_g(t) + I_d(t)$$
$$0 \le I_g(t) \le I_{g_{MAX}}$$
$$I_{d_{MIN}} \le I_d(t) \le I_{d_{MAX}}$$
$$0 < SOC_{\min} \le SOC \le SOC_{\max} \le 1$$

where $\dot{m}_{f,ICE}$ is fuel flow rate from IC engine, $\dot{m}_{f,Batt,eq}$ is the equivalent fuel consumption of battery pack, I_g, I_d and I_{load} are genset current, DC/DC converter output current and load current, respectively. In the following, we will discuss the objective function formulations for two versions of ECMS.

Constant ECMS

In this version of ECMS, the equivalent fuel consumption of the battery can be formulated based on the battery power, battery efficiency, and lower heating value of the fuel as follows [19]:

$$\dot{m}_{f,eq} = \dot{m}_{f,ICE}(I_{load} - I_d) + \qquad (6)$$
$$s \left(\frac{\gamma}{\eta_{el,dis}(I_d)} + (1-\gamma)\eta_{el,chg}(I_d) \right) \frac{I_d V_g}{Q_{LHV}} p(SOC)$$

where $\gamma = 1$ for $I_d \ge 0$ and $\gamma = 0$ otherwise and s is a constant tunable equivalence factor, $\eta_{el,chg}$ and $\eta_{el,dis}$ are the charging and discharging efficiency of the electrical path to/from the batteries, and V_g is the load voltage at the electrical

summation. Notice that a penalty function $p(SOC)$ is used here to take care of the SOC variation within the desired SOC band. In this paper, we used the following penalty function [4]:

$$p(SOC) = 1 - \left(\frac{SOC - \frac{1}{2} SOC_{ref}}{\frac{SOC_{MAX} - SOC_{MIN}}{2}} \right)^3 \qquad (7)$$

However, in constant ECMS the performance strongly depends on the choice of the value of the equivalence factor s. Moreover, a value of s suitable for a given driving cycle may lead to poor performance for other driving cycles. Although the penalty function tries to manage SOC variation, it may not be effective and it also depends on the choice of the penalty function [11].

Making the equivalence factor s time-varying and adaptive based on the SOC of the battery could remove these drawbacks [10]. This version of the ECMS strategy is called adaptive ECMS and is discussed next.

Adaptive ECMS

In adaptive ECMS [12], the equivalent fuel consumption of the battery can be formulated as follows:

$$\dot{m}_{f,eq} = \dot{m}_{f,ICE}(I_{load} - I_d) + \qquad (8)$$
$$s \left(\frac{\gamma}{\eta_{el,dis}(I_d)} + (1-\gamma)\eta_{el,chg}(I_d) \right) \frac{I_d V_g}{Q_{LHV}}$$
$$s_k = \frac{s_{k-1} + s_{k-2}}{2} + k_p (SOC_{ref} - SOC(t))$$
where $\quad t = kT, k = 0,1,2,...$

and s_k is time varying equivalence factor and is updated in every T seconds, k_p is constant feedback gain to be chosen. In adaptive ECMS, feedback of SOC is used to refresh the control parameters making it more stable and less sensitive to the choice of an initial equivalence factor. However, the performance of the adaptive ECMS depends on the choice of the tunable parameters k_p and T.

RESULTS AND DISCUSSIONS

In this section, application of the HIL platform is demonstrated using a Federal Urban Driving Schedule (FUDS) driving cycle experiment. Due to power limitations in the HIL platform (low power components were used in this design), a scaled down version of the power requirements of the FUDS cycle (20% of original) were considered.

Results for two different cases are presented: one for constant ECMS and another one for adaptive ECMS. The tuning parameter for constant ECMS is $s = 0.0001$. For adaptive ECMS, we used $k_p = 0.001$ and $T = 50$ seconds. Performances of these two control strategies are shown in Figure 8.

5

In both cases, the power requirement is met by dividing the current between genset and battery sources as shown in Figure 8 (for a zoomed-in time window of the cycle). Both versions seem to operate comparably in these plots. However, there are major differences on their performance over the long run.
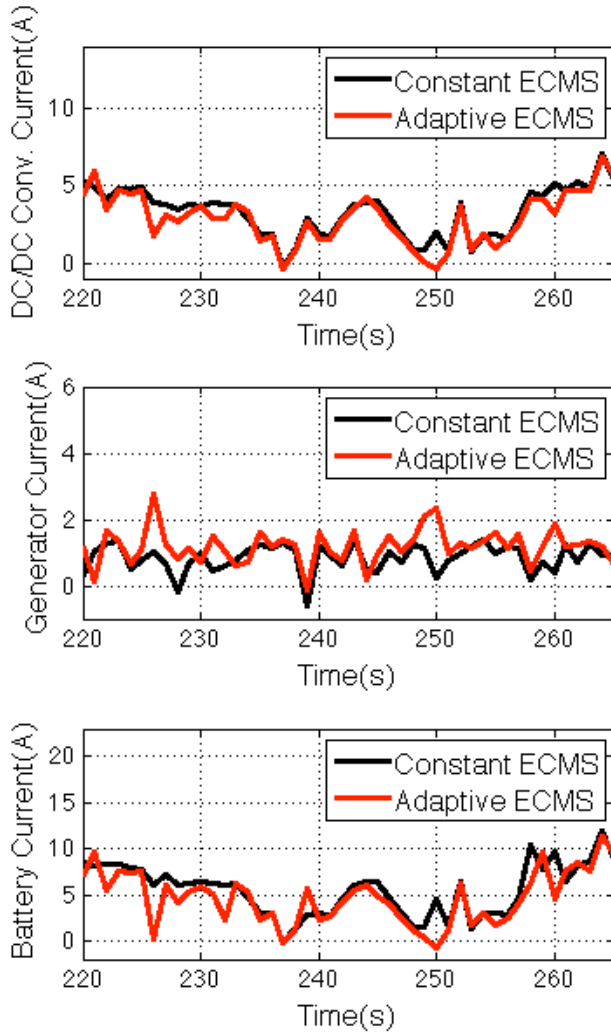

Figure 8: Zoomed in View of Current Profiles During a Portion of the FUDS Cycle

The ratio of the current allocation to the battery and genset is determined by the value of equivalence factor s. It is expected that, since s is the cost of battery power versus genset power, the larger s is, the more the genset is used to fulfill the current demand from the load (drive cycle). Figure 9 shows that the adaptive ECMS uses larger values of s during the drive cycle than the constant ECMS. This leads to less usage of battery in the case of adaptive ECMS. It is also evident from Figure 10 that the battery pack is used less in adaptive ECMS because SOC remains higher. With adaptive ECMS, the larger value of s in the control strategy causes the genset to work even harder and produce more current to meet total load current demand. At the same time, the battery current is reduced. At the power split, the battery is contributing the majority of current demand for both constant and adaptive ECMS (see Figure 8). The reason behind more usage of battery than genset lies in our particular selection of design parameter s for constant ECMS and design parameters k_p and T for adaptive ECMS. This results in low genset current demand leading to low genset efficiencies for both constant and adaptive ECMS (the reader may refer to the genset efficiency map given in Figure 3). The histogram of genset efficiency points during the FUDS cycle for both constant and adaptive ECMS are shown in Figure 11. Careful observation shows that in case of adaptive ECMS there is a larger frequency of higher efficiency points than in constant ECMS. Although this difference is minute in one drive cycle, multiple repetitions of the drive cycle would result in better and significant fuel economy for adaptive ECMS.
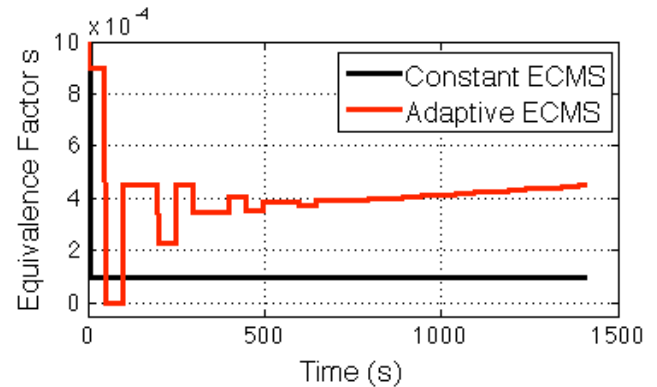

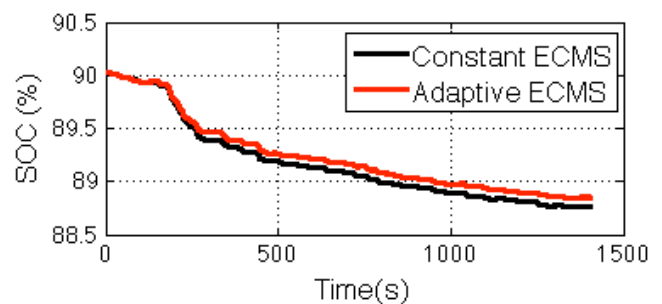**Figure 9: Equivalence Factor During FUDS Cycle**

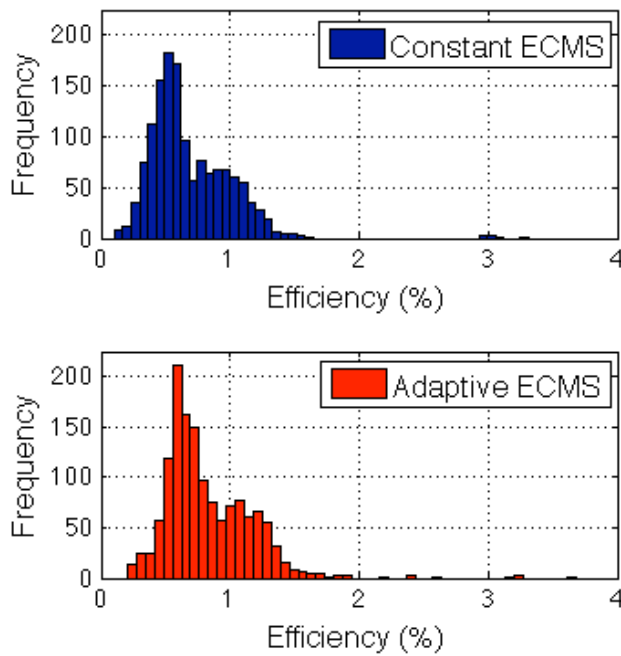**Figure 10: Battery SOC During FUDS Cycle**

6

Copyright © 2014 by ASME

Figure 11: Histogram of Genset Efficiencies for FUDS Cycle

	$m_{f,eq}$ (g)
Constant ECMS	255
Adaptive ECMS	252

Table 2: FUDS Cycle Gasoline Fuel Consumption with Constant and Adaptive ECMS

Table 2 shows adaptive ECMS minimizes the total $m_{f,eq}$ better than constant ECMS, as expected. Note that over many repeats of the cycle, these differences become substantial.

CONCLUSION

In this paper, we described a HIL setup for series hybrid powertrain testing and evaluation. The setup was built from off-the-shelf components for educational and research purposes. Details for hardware and control system integration were discussed. We discussed two successful implementations of two versions of the ECMS along with experimental results.

Further improvements to the platform have yet to be completed. For example, more accurate models of components can be used in lieu of the simplified models used here. Other control strategies can also be readily implemented and evaluated.

NOMENCLATURE

ρ	density of air
m	vehicle mass
m_{eff}	effective vehicle mass
A_f	frontal area
g	gravitational acceleration
C_d	coefficient of drag
C_r	coefficient of rolling resistance
V_b	single battery voltage
V_g	genset voltage
V_{oc}	open circuit voltage of single battery
V_d	DC/DC converter output voltage
R	resistance of single battery
I_b	battery pack current
I_d	DC/DC converter output current
I_{load}	DC load current
I_g	genset current
V_{ref}	DC/DC converter reference voltage
Temp	temperature of battery
SOC	battery state of charge
SOC_{ref}	reference state of charge
k_p	constant feedback gain for adaptive ECMS
s	equivalence factor
s_k	equivalence factor at k time step
s_{k-1}	equivalence factor at previous time step
s_{k-2}	equivalence factor at two previous time steps
T	adaptive ECMS update time
J	objective function
P_{req}	total power requirement
P_{gen}	genset power
P_{el}	battery power
$m_{f,eq}$	equivalent fuel consumption
$\dot{m}_{f,eq}$	equivalent fuel flow rate
$\dot{m}_{f,ICE}$	genset fuel flow rate
$\dot{m}_{f,Batt,eq}$	equivalent battery fuel flow rate
$\eta_{el,dis}$	battery pack discharge efficiency
$\eta_{el,chg}$	battery pack charge efficiency
Q_{LHV}	gasoline lower heating value

REFERENCES

[1] A. G. Boulanger, A. C. Chu, S. Maxx, and D. L. Waltz, "Vehicle Electrification: Status and Issues," Proceedings of the IEEE, vol. 99, no. 6, pp. 1116-1138, 2011.

[2] C. C. Lin, J. M. Kang, J. W. Grizzle, and H. Peng, "Energy management strategy for parallel hybrid electric truck," in Proc. Amer. Control Conf., 2001, pp. 2878–2883.

[3] M. Salman, N. J. Schouten, and N. A. Kheir, "Control strategies for parallel hybrid vehicles," in Proc. Amer. Control Conf., 2000, pp. 524–528.

[4] G. Paganelli, G. Ercole, A. Brahma, Y. Guezennec, and G. Rizzoni, "General supervisory control policy for the energy optimization of charge-sustaining hybrid electric vehicles," J. SAE Rev., vol. 22, pp. 511–518, 2001.

[5] H. Fathy, Z. Filipi, J. Hagena, and J. Stein, "Review of Hardware-in-the-Loop Simulation and Its Prospects in the Automotive Area," in Proc. SPIE Int Soc Opt Eng, vol. 6228, 2006.

[6] R. Trigui, , Bron ; B. Jeanneret, ; B. Malaquin, F. Badin, "Hardware In the Loop Simulation of a Diesel Parallel Mild-Hybrid Electric Vehicle," Vehicle Power and Propulsion Conference, 2007.

[7] O. Grondin, P. Moulin, A. Chasse, and A. Sciarretta, "Energy management strategy for Diesel hybrid electric vehicle," Vehicle Power and Propulsion Conference, 2011.

[8] C. Du, F. Yan, X. Hou, and J. Hu "Development Platform for the Control System of Hybrid Electric Vehicles Powertrain," Asia-Pacific Power and Energy Engineering Conference, 2010.

[9] J. Wu, C. Dufour, and L. Sun, "Hardware-in-the-Loop Testing of hybrid vehicle motor drives at Ford Motor Company," Vehicle Power and Propulsion Conference, 2010.

[10] C. Musardo, G. Rizzoni, Y. Guezennec, and B. Staccia, "A-ECMS: An adaptive algorithm for hybrid electric vehicle energy management," Eur. J. Control, vol. 11, no. 4–5, pp. 509–524, 2005.

[11] P. Pisu, and G. Rizzoni. "A comparative study of supervisory control strategies for hybrid electric vehicles." Control Systems Technology, IEEE Transactions on 15.3 (2007): 506-518.

[12] S. Onori, L. Serrao, and G. Rizzoni. "Adaptive equivalent consumption minimization strategy for hybrid electric vehicles." In ASME 2010 Dynamic Systems and Control Conference, pp. 499-505. American Society of Mechanical Engineers, 2010.

[13] Honda 2.5kW Generator, Model EN2500. http://cdn.powerequipment.honda.com/pe/pdf/manuals/31ZT2602.pdf

[14] Werker 35Ah 12V Sealed Lead Acid Battery. http://www.batteriesplus.com/product/32627-WKA12--35C-12-Volt-35Ah-Werker-Battery/100085-1/102629-SLA-Sealed-Lead-Acid-Batteries/102645-Werker/12V.aspx

[15] Technology Dynamics Inc., Unidirectional AC/DC converter, Model TDRSP-1500-48, http://www.technologydynamicsinc.com/switching/tdrsp1500-48.php

[16] Zahn Inc., Bidirectional DC/DC converter, Model DC6336-SU, http://www.zahninc.com/su4x590to2000W.html

[17] NH Research, High-Current DC Load, Model 4700 Series, http://www.nhresearch.com/Products/4700_load.htm

[18] Michigan Scientific., Slip Ring Assembly, Model SR10M/E60, http://www.michsci.com/Products/sliprings/eos/sr10m_e60.htm

[19] P. Pisu, G. Rizzoni, "A supervisory control strategy for series hybrid electric vehicles with two energy storage systems," Vehicle Power and Propulsion, 2005 IEEE Conference , vol., no., pp.8 pp.,, 7-9 Sept. 2005.